Monitoring Disturbances in Smart Grids Using Distributed Sequential Change Detection

Shang Li
Electrical Engineering Department
Columbia University, New York, NY 10025
Email: shang@ee.columbia.edu

Xiaodong Wang
Electrical Engineering Department
Columbia University, New York, NY 10025
Email: wangx@ee.columbia.edu

***Abstract*—This paper considers the online disturbance detection in smart grids by using multiple sensors, which sample the power signal and communicate wirelessly to a fusion center that detects the occurrence of abnormal disturbance. Under the sequential change detection framework, we first introduce a generalized local likelihood ratio (GLLR) detector based on an autoregressive model for the disturbance. Then we propose a decentralized GLLR detector, where each sensor computes its own GLLR statistic, adaptively samples them using a level-triggered sampling scheme, and transmits the samples to the fusion center. The proposed decentralized disturbance detection scheme substantially lowers the communication overhead, while its performance is close to that of the centralized scheme.**

I. Introduction

Nowadays the power quality has become a critical concern for the emerging smart grids, due to the rapidly growing number of equipments that not only generate but also are sensitive to various disturbances. One crucial task is the real-time detection of power quality disturbance in the process of observing either the voltage or the current signal. In this paper, we focus on the voltage disturbance while the method for detecting current disturbance follows similarly. A voltage disturbance consists of any deviation of the actual voltage signal from the nominal sinusoidal waveform with prescribed amplitude and frequency. The real-time disturbance detection enables the power system to promptly respond to the detrimental fluctuations caused by the generator and load operations, abrupt environment change (e.g., lightning strike), etc. Moreover, it also triggers the abnormal data recording, which helps electricity providers to perform off-line assessment. However, the monitored data in practice are always corrupted by noise, which could deteriorate the detection performance, leading to frequent false alarms or large decision delay. The fundamental goal is to detect the disturbance from the noisy observed voltage signal as soon as possible after its occurrence, so that certain protection measures can be taken in time before any severe damage is incurred and/or the data recording process is activated immediately.

Thus far, one of the most widely used disturbance detection methods is by monitoring the root mean square (RMS) sequence, which is computed over a sliding window of length W (usually half-cycle of the nominal waveform) as $Q(n) = \sqrt{\frac{1}{W}\sum_{k=n-W+1}^{n} y_k^2}$, where y_k is the kth sample of the voltage waveform. A disturbance is detected once the RMS exceeds a prescribed threshold. However, since no statistical property of the observed waveform is exploited, the RMS method is inefficient for the noisy observations. In addition, the time resolution of the detection is decreased by the window for computing RMS. Other methods detect the distortion in the frequency domain, mainly by the wavelet transform or the short-time Fourier transform [1]. These methods are limited by the size of the window over which the transformation is performed, and they are less effective in the presence of noise. A promising approach to mitigate the noise is to employ the statistical framework of hypothesis testing. In [2], the likelihood ratio test are employed to de-noise the wavelet transform coefficients, which is a fixed-sample size approach rather than a sequential one, thus is inefficient in terms of time resolution. In [3], under the sequential change detection framework, a weighted CUSUM test was introduced, by examining the different distributions of the observed waveforms before and after the occurrence of the disturbance. However, the disturbance signal is assumed to be independent over time.

In this paper, we also formulate the online voltage monitoring as a sequential change detection problem. But compared to [3], we build our framework on the autoregressive (AR) model, which captures the time correlation of the disturbance, and thus provides more realistic characterization. Moreover, we consider the scenario where multiple sensors are employed for monitoring the voltage waveform and they communicate wirelessly with a fusion center, which is responsible for making decisions. In particular, deploying multiple sensors provides diversity across the sensors, thus enables quicker detection of the occurrence of the disturbance.

The reminder of this paper is organized as follows. In Section II, we introduce the generalized local likelihood ratio (GLLR) change detection scheme based on the AR model. In Section III, we propose the decentralized GLLR test based on the level-triggered sampling. Simulation results are provided in Section IV.

II. GLLR Sequential Detection Scheme

Suppose there are L sensors that communicate with a fusion center, which makes the decision on change occurrence. Without loss of generality, we assume that the disturbance occurs at some unknown time t_0. That is, before t_0 the voltage waveform is a sinusoid with the nominal magnitude, frequency and phase: $f_n^{\text{nominal}} = a_0 \sin(2\pi f_0 n + \phi_0)$. After t_0, the disturbance distorts the nominal sinusoid. Assuming that the parameters $\{a_0, f_0, \phi_0\}$ take prescribed values, we can subtract the nominal waveform from the measurement to isolate the disturbance components from the noisy observed signal [3]. That is, the observed signal after pre-processing before the disturbance occurs consists of white Gaussian noise:

$$y_n^{(\ell)} = \nu_n^{(\ell)} \sim \mathcal{N}(0, \sigma_\nu^2), \quad n < t_0, \quad \ell = 1, 2, \ldots, L, \quad (1)$$

where $y_n^{(\ell)}$ is the observation from the ℓth sensor at time n. It is assumed that the noise is independent in time and across sensors. On the other hand, with the subtraction of the nominal sinusoid, the observed waveform after t_0 consists of only disturbance and noise. Following [4], we use an AR model to characterize the disturbance signal, which is popular in analyzing the spectral property of various types of signals, such as speech signals [5] and seismic signals [6]. The AR model is able to represent a broad spectral range, yielding robust characterization of a variety of potential disturbances; whereas the sinusoidal model (i.e., modeling the disturbance signal as a sum of sinusoids) in [3, 7] only represents a fixed number of certain frequency components. Specifically, the observed waveform after t_0 at the sensors is expressed in the following AR formula:

$$y_n^{(\ell)} = \sum_{j=1}^{p} a_j y_{n-j}^{(\ell)} + u_n^{(\ell)}, \quad n > t_0, \quad \ell = 1, 2, \ldots, L, \quad (2)$$

where $u_n^{(\ell)} \sim \mathcal{N}(0, \sigma_u^2)$ is the driving noise of the AR process, accounting for the excitation of the disturbance and the measurement noise.

Denoting the parameter vector comprised of the AR coefficients and the variance as $\boldsymbol{\theta}$, then the disturbance-induced waveform change in (1) and (2) corresponds to the change of the parameter vector at $n = t_0$ from $\boldsymbol{\theta} = \boldsymbol{\theta}_0 \triangleq [0, 0, \ldots, 0, \sigma_\nu]^\intercal$ to $\boldsymbol{\theta} = \boldsymbol{\theta}_1 \triangleq [a_1, a_2, \ldots, a_p, \sigma_u]^\intercal$. Defining $\mathbf{y}_j^{k(\ell)} \triangleq [y_k^{(\ell)}, y_{k-1}^{(\ell)}, \ldots, y_j^{(\ell)}]^\intercal$, the log-likelihood ratio of samples from time j to k is expressed as [8, Ch.8]

$$S_j^k = \sum_{\ell=1}^{L}\sum_{i=j}^{k} s_i^{(\ell)}, \quad s_i^{(\ell)} \triangleq \frac{1}{2}\log\frac{\sigma_\nu^2}{\sigma_u^2} - \frac{\varepsilon_{i,\boldsymbol{\theta}_1}^{(\ell)}{}^2}{2\sigma_u^2} + \frac{\varepsilon_{i,\boldsymbol{\theta}_0}^{(\ell)}{}^2}{2\sigma_\nu^2}, \quad (3)$$

with $\varepsilon_{n,\boldsymbol{\theta}_0}^{(\ell)} \triangleq y_n^{(\ell)}$ and $\varepsilon_{n,\boldsymbol{\theta}_1}^{(\ell)} \triangleq y_n^{(\ell)} - \sum_{j=1}^{p} a_j y_{n-j}^{(\ell)}$. However, this log-likelihood ratio (3) cannot be directly applied to the sequential change detection since the post-change parameter $\boldsymbol{\theta}_1$ cannot be specified due to the diverse nature of the disturbance. To overcome this problem, we apply the generalized local log-likelihood ratio (GLLR) test.

The GLLR test is derived by combining the local assumption and the generalized likelihood ratio approach. The former assumes that the parameter change is small, i.e., $\boldsymbol{\theta}_1 \approx \boldsymbol{\theta}_0$. The corresponding test under this assumption is called the locally optimal test, meaning that the detector is asymptotically optimal as $\mathbf{r} \triangleq \boldsymbol{\theta}_1 - \boldsymbol{\theta}_0 \to \mathbf{0}$. Since that we have no prior knowledge of the disturbance, assuming that the change is small corresponds to the worst-case scenario that is most difficult to detect. On the other hand, the significant changes induced by the disturbance can be easily detected by any simple detection schemes. To that end, using the local assumption, we approximate the log-likelihood ratio by a linear expansion (up to the second order) around $\boldsymbol{\theta}_0$:

$$S_j^k \approx \mathbf{r}^\intercal \left(\sum_{\ell=1}^{L}\sum_{i=j}^{k} \mathbf{z}_i^{(\ell)}\right) - \frac{1}{2}\mathbf{r}^\intercal \left(\sum_{\ell=1}^{L}\sum_{i=j}^{k} \mathbf{w}_i^{(\ell)}\right)\mathbf{r}, \quad (4)$$

with $\mathbf{z}_i^{(\ell)}$ and $\mathbf{w}_i^{(\ell)}$ given by (5) at the top of next page. Here $\mathbf{r}$ is a small vector (i.e., $\mathbf{r}^\intercal\mathbf{r}$ is small).

Then the generalized likelihood ratio approach decides the change direction $\mathbf{r}$ in (4) by substituting $\mathbf{r}$ with its maximum-likelihood estimate, i.e., $\tilde{S}_j^k = \sup_{\mathbf{r}} S_j^k$. Recalling that $\boldsymbol{\theta}_1 \approx \boldsymbol{\theta}_0$, we have

$$\sum_{\ell=1}^{L}\sum_{i=j}^{k} \frac{\mathbf{w}_i^{(\ell)}}{L(k-j+1)} \to \mathbf{J} \triangleq \mathbb{E}_{\boldsymbol{\theta}_0}(\mathbf{w}_i^{(\ell)}) = \begin{bmatrix} \mathbf{I} & \mathbf{0} \\ \mathbf{0} & \frac{2}{\sigma_\nu^2} \end{bmatrix}, \quad (6)$$

as $L(k-j+1) \to \infty$, corresponding to the case of either large number of samples, and/or large number of sensors. Here $\mathbf{I}$ is the $p \times p$ identity matrix. We constrain $\mathbf{r}$ to be on a small ellipse $\mathbf{r}^\intercal\mathbf{J}\mathbf{r} = b^2$, where b is a small radius parameter, and evaluate the generalized local likelihood ratio as

$$\begin{aligned} \tilde{S}_j^k &= \sup_{\mathbf{r}^\intercal\mathbf{J}\mathbf{r}=b^2} \mathbf{r}^\intercal \left(\sum_{\ell=1}^{L}\sum_{i=j}^{k} \mathbf{z}_i^{(\ell)}\right) - \frac{L(k-j+1)}{2}\mathbf{r}^\intercal\mathbf{J}\mathbf{r} \\ &= bU_j^k - \frac{L(k-j+1)}{2}b^2, \end{aligned} \quad (7)$$

with $\tilde{\mathbf{z}}_i^{(\ell)} \triangleq \left(\mathbf{J}^{1/2}\right)^{-1}\mathbf{z}_{\mathbf{i}}^{(\ell)}$ and

$$U_j^k \triangleq \sqrt{\left(\sum_{\ell=1}^{L}\sum_{i=j}^{k} \tilde{\mathbf{z}}_i^{(\ell)}\right)^\intercal \left(\sum_{\ell=1}^{L}\sum_{i=j}^{k} \tilde{\mathbf{z}}_i^{(\ell)}\right)}. \quad (8)$$

With (7) available, then the occurrence of the disturbance can be detected using the following sequential change detection algorithm:

$$N_k = N_{k-1}\mathbb{1}_{\{\tilde{g}_{k-1}>0\}} + 1, \quad (9)$$

$$\tilde{g}_k = \left(\tilde{S}_{k-N_k+1}^k\right)^+, \quad \tilde{T} = \inf\{k : \tilde{g}_k \geq h\}. \quad (10)$$

which is an equivalent form of the well-known Page's CUSUM procedure, but based on the GLLR statistic. Note that $x^+ \triangleq \max\{x, 0\}$. Due to the space limitation, we refer to [8, Ch.2] for detailed description of this procedure. Here N_k is the number of observations at time k since the last time of resetting the test statistic $\tilde{g}_k$ to zero at time $k - N_k$ and $\mathbb{1}_{\{\cdot\}}$ is the indicator function. Note that at each time k, g_k is computed and compared with the threshold h, which is choosen to meet the false alarm constraint. $\tilde{T}$ is the first time that $\tilde{g}_k$ exceeds h and when the disturbance is declared to occur.

III. Decentralized Scheme Using Level-triggered Sampling

The detection scheme discussed in the previous section is essentially a centralized one, because the signals observed at different sensors are assumed available to the fusion center. However, in practice, the sensors are equipped with limited power storage, and bandwidth-limited communication capability. Therefore, in designing a practical system, we need to consider the *rate constraint* (i.e., the sensors should communicate with the fusion center at a lower rate than their local sampling rate) and the *quantization constraint* (i.e., each sensor should transmit a small number of bits every time it communicates with the fusion center). Thus the decentralized detection, where the sensors communicate with the fusion center in some low-rate fashion, becomes necessary. In this section, we propose a decentralized scheme based on the level-triggered sampling, which efficiently lowers the communication overhead in terms of both the communication frequency and the number of information bits at each transmission.

$$\mathbf{z}_i^{(\ell)} \triangleq \frac{\partial s_i^{(\ell)}}{\partial \boldsymbol{\theta}_1}\Big|_{\boldsymbol{\theta}_1=\boldsymbol{\theta}_0} = \begin{bmatrix} \frac{1}{\sigma_\nu^2} y_i^{(\ell)} \mathbf{y}_{i-p}^{i-1(\ell)} \\ \frac{1}{\sigma_\nu}\left(\frac{y_i^{(\ell)2}}{\sigma_\nu^2}-1\right) \end{bmatrix}, \qquad \mathbf{w}_i^{(\ell)} \triangleq -\frac{\partial^2 s_i^{(\ell)}}{\partial \boldsymbol{\theta}_1^2}\Big|_{\boldsymbol{\theta}_1=\boldsymbol{\theta}_0} = \begin{bmatrix} \mathbf{y}_{i-p}^{i-1(\ell)}\mathbf{y}_{i-p}^{i-1(\ell)\mathsf{T}} & \frac{2y_i^{(\ell)}}{\sigma_\nu}\mathbf{y}_{i-p}^{i-1(\ell)} \\ \frac{2y_i^{(\ell)}}{\sigma_\nu}\mathbf{y}_{i-p}^{i-1(\ell)\mathsf{T}} & \frac{3y_i^{(\ell)2}}{\sigma_\nu^2}-1 \end{bmatrix} \tag{5}$$

In the decentralized setup, the goal is first to select an efficient communication scheme, then the fusion center performs the detection based on information sent by sensors. Before proceeding, we first introduce an asymptotic transformation to the centralized statistic in (7) as follows:

$$\tilde{S}_j^k \to \sum_{\ell=1}^{L} \tilde{S}_{k-N_k+1}^{k,(\ell)} \triangleq \sum_{\ell=1}^{L}\left(bV_j^{k(\ell)} - \frac{k-j+1}{2}b^2\right), \tag{11}$$

where $V_j^{k(\ell)} \triangleq \sqrt{\left(\sum_{i=j}^{k}\tilde{\mathbf{z}}_i^{(\ell)}\right)^{\mathsf{T}}\left(\sum_{i=j}^{k}\tilde{\mathbf{z}}_i^{(\ell)}\right)}$, as $k-j+1 \to \infty$. In essence, the statistic in (11) can be interpreted as that each sensor estimates the change direction $\mathbf{r}$ locally. The above asymptotic result enables the sensors to compute the local statistic $\tilde{S}_{k-N_k+1}^{k,(\ell)}$ individually based on their own observations, instead of quantizing and transmitting the observations at every local sampling instant to the fusion center. Such an approximation as (11) is beneficial for decentralizing the GLLR test, which as we will see later, on one hand, lowers the communication overhead between sensors and the fusion center; on the other hand, it also decreases the computation burden at the fusion center, which now only needs to sum up the received statistics from sensors to recover the global statistic. In what follows, we build on (11) to develop an efficient decentralized implementation based on the level-triggered communication scheme at the sensors and its associated decision rule at the fusion center.

The level-triggered sampling strategy is essentially a single-bit quantization of the local statistic, where the transmission of the local statistic is only triggered once it hits a certain value, thus is observation-adaptive. Moreover, all sensors communicate with the fusion center asynchronously, which avoids the use of a global clock for synchronization. We begin by simplifying the notation of the local test statistic at the ℓth sensor $\{\tilde{S}_{k-N_k+1}^{k,(\ell)}\}$ as $\{\tilde{S}_k^{(\ell)}\}$, because N_k is uniquely determined by k, and denoting the nth communicating time of the ℓth sensor as k_n^ℓ. Note that at the ℓth sensor, we can decompose the test statistic as $\tilde{S}_k^{(\ell)} = \tilde{S}_k^{(\ell)} - \tilde{S}_{k_{n-1}^\ell}^{(\ell)} + \tilde{S}_{k_{n-1}^\ell}^{(\ell)} - \ldots - \tilde{S}_{k_1^\ell}^{(\ell)} + \tilde{S}_{k_1^\ell}^{(\ell)} - \tilde{S}_0^{(\ell)}$, where $\tilde{S}_0^{(\ell)} = 0$, and the transmission instants k_n^ℓ is recursively defined as

$$k_n^\ell \triangleq \inf\left\{k > k_{n-1}^\ell : \tilde{S}_k^{(\ell)} - \tilde{S}_{k_{n-1}}^{(\ell)} \notin (-\underline{\Delta}, \overline{\Delta})\right\}, \tag{12}$$

with $k_0^\ell = 0$, $\tilde{S}_0^{(\ell)} = 0$, $\overline{\Delta}$ and $\underline{\Delta}$ are positive constants, selected to control the frequency of transmission. Note that since it is assumed that the observations at different sensors follow the same distribution, $\overline{\Delta}$ and $\underline{\Delta}$ take the same values across the sensors, and they are also known to the fusion center. According to (12), each sensor informs the fusion center of its local statistic every time it cumulates to exit the interval $[-\underline{\Delta}, \overline{\Delta}]$. Assuming that $\tilde{S}_{k_n^\ell}^{(\ell)} - \tilde{S}_{k_{n-1}^\ell}^{(\ell)}$ hits the boundary exactly in (12), we have $\tilde{S}_{k_n^\ell}^{(\ell)} - \tilde{S}_{k_{n-1}^\ell}^{(\ell)} = -\underline{\Delta}$ or $\overline{\Delta}$. Then the local statistic can be delivered by sending only one-bit information of which boundary is hit to the fusion center. In particular, the nth one-bit message transmitted by the ℓth sensor is given by

$$x_n^{(\ell)} = \begin{cases} 1, & \text{if } \tilde{S}_{k_n^\ell}^{(\ell)} - \tilde{S}_{k_{n-1}^\ell}^{(\ell)} \ge \overline{\Delta}, \\ -1, & \text{if } \tilde{S}_{k_n^\ell}^{(\ell)} - \tilde{S}_{k_{n-1}^\ell}^{(\ell)} \le -\underline{\Delta}. \end{cases} \tag{13}$$

In essence, the above communication scheme implies that the fusion center adaptively samples the local statistic at all sensors to lower the transmission frequency. Moreover, the quantization of local statistic is no longer needed, which substantially decreases the amount of data at each transmission. The level-triggered sampling scheme at each sensor is summarized as Algorithm 1. Note that the reset signal in the procedure corresponds to the indicator function in the GLLR test (9): recalling that N_k is the number of observations for computing the local statistic, when the global statistic at the fusion center $\tilde{S}_k \le 0$, a reset signal is broadcast to all sensors informing them to reset $N_k = 1$; otherwise, with no reset signal, N_k keeps increasing. The above transmission scheme features an inherent data compression and adaptive communication between the sensors and the fusion center. Moreover, the one-bit transmission induces significant savings in bandwidth and transmission power.

Algorithm 1 : Level-triggered sampling of the GLLR statistic at the ℓth sensor

1: Initialization: $k \leftarrow 0$
2: Reset: $\lambda \leftarrow 0, N \leftarrow 1$
3: **while** $\tilde{S}_{k-N+1}^{k,(\ell)} - \lambda \in (-\underline{\Delta}, \overline{\Delta})$ **do**
4: $\quad k \leftarrow k+1$
5: $\quad$ Check the reset signal broadcasted by the fusion center:
6: $\quad$ **if** present **then**
7: $\quad\quad$ go to line 2
8: $\quad$ **else**
9: $\quad\quad N \leftarrow N+1$
10: $\quad$ **end if**
11: $\quad$ Compute $\tilde{S}_{k-N+1}^{k,(\ell)}$ by (11)
12: **end while**
13: Send $x_k^{(\ell)} = \text{sign}(\tilde{S}_{k-N+1}^{k,(\ell)} - \lambda)$ to the fusion center
14: $\lambda \leftarrow \tilde{S}_{k-N+1}^{k,(\ell)}$
15: Check the reset signal broadcast by the fusion center:
16: $\quad$ **if** present **then** go to line 2
17: $\quad$ **else** go to line 3.

On the other side, the fusion center receives the information bits from each sensor asynchronously and updates the global running statistic as follows:

$$\tilde{S}_k = \tilde{S}_{k-1} + \sum_{\ell=1}^{L}\left(\mathbb{1}_{\{k=k_n^\ell,\, x_n^{(\ell)}=1\}}\overline{\Delta} - \mathbb{1}_{\{k=k_n^\ell,\, x_n^{(\ell)}=-1\}}\underline{\Delta}\right). \tag{14}$$

Every time the global statistic is updated at the fusion center, it is used to perform the GLLR test given by (9)-(10). There

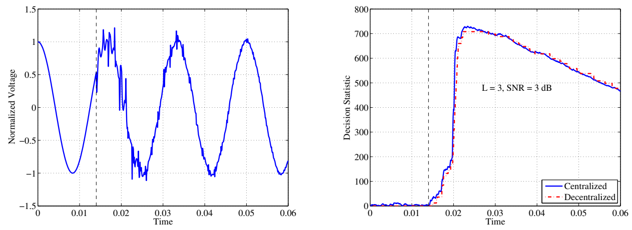

Fig. 1. Detection of the typical voltage disturbance using the proposed centralized and decentralized GLLR detectors.

are two decisions to make, i.e., triggering the alarm that a disturbance is detected or continuing to receive more information bits from the sensors.

In summary, through the level-triggered sampling scheme, we efficiently recover the decision statistic at the fusion center by collecting local statistics from sensors. Specifically, compared to the centralized setup where observations are transmitted at every sampling instant with multiple quantization bits, the level-triggered sampling features lower communication frequency (which can be controlled by the parameters $\underline{\Delta}$ and $\overline{\Delta}$) and one-bit representation of each sample.

IV. Simulation Results

In this section, we numerically examine the performance of both the centralized and level-triggered sampling based decentralized GLLR tests. Throughout this section, the GLLR detector is implemented based on second-order AR model. We first apply the proposed tests on a typical voltage disturbance induced by capacitor switching. The voltage disturbance data here is obtained by the Alternative Transients Program (ATP-EMTP) software [9]. The nominal voltage is a sinusoidal waveform with $f_0 = 60$Hz and unit magnitude. Three sensors are deployed in the detection system, each of which samples the voltage waveform at a rate of 20KHz. In Fig. 1, we plot both the signals before and after the occurrence of the disturbance (on the left), and the decision statistic $\tilde{g}_k$ at the fusion center as a function of time (on the right). The starting point of the disturbance is marked by a dashed line. We see that the decision statistics at the fusion center exhibit abrupt changes on the occurrence of the disturbance. Note that both the centralized decision statistic and the decentralized one are shown (the interval $[-\underline{\Delta}, \overline{\Delta}]$ is designed such that $\mathbb{E}_{\boldsymbol{\theta}_0}(\tau) = 10$ samples, where τ denotes the communication interval) and they match closely with each other.

Next, to perform a rigorous comparison with the conventional RMS method and also to compare the proposed centralized and decentralized solutions, the mean detection delay versus the false alarm probability is examined. Since the ATP-EMTP simulated disturbance data is based on transient model and is highly non-stationary, thus it is unsuitable for performance evaluation from the signal processing point of view. To that end, we use Matlab simulated data to simplify the disturbance as a non-transient sinusoidal waveform with fixed frequency of 500Hz added to the nominal waveform, which is also employed as "synthetic data" in [1]. We first consider the single-sensor case and compare the performance of the proposed GLLR test and that of the RMS method. Here the RMS is implemented with a half-cycle window

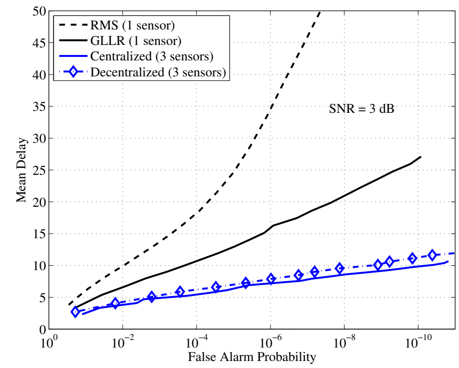

Fig. 2. The detection delay versus the false alarm probability for various detectors.

that slides point by point, achieving the best possible time resolution. It is seen from Fig. 2 that the proposed GLLR test significantly outperforms the RMS method as the false alarm probability becomes smaller. Then we consider the case where there are three sensors, and the performances of the centralized GLLR detector and the decentralized detector are also shown in Fig. 2. Compared with the single-sensor case, it is seen that employing multiple sensors substantially improves the performance in terms of achieving a much shorter detection delay. The local thresholds for the level-triggered sampling is chosen as $[-\underline{\Delta}, \overline{\Delta}] = [-5.4, 5.4]$, under which at each sensor we have $\mathbb{E}_{\boldsymbol{\theta}_0}(\tau) = 15$ samples and $\mathbb{E}_{\boldsymbol{\theta}_1}(\tau) = 2.5$ samples. It is seen that the proposed decentralized detector only exhibits a small increase of detection delay compared to the centralized detector, while significantly saving the communication overhead between the sensors and the fusion center by sending one-bit sequence at every level-triggered sampling instant.

References

[1] M. H. J. Bollen and I. Y. H. Gu, *Signal processing of power quality disturbances*. Hoboken, NJ: Wiley-IEEE Press, 2006.

[2] U. D. Dwivedi and S. N. singh, "Denoising techniques with change-point approach for wavelet-based power-quality monitoring," *IEEE Trans. Power Del.*, vol. 24, no. 3, pp. 1719–1727, July 2009.

[3] X. He, M.-O. Pun, C.-C. Kuo, and Y. Zhao, "A change-point detection approach to power quality monitoring in smart grids," in *Proc. IEEE International Workshop on Smart Grid Communication*, Cape Town, South Africa, May 2010.

[4] I. Y. H. Gu, M. H. J. Bollen, and E. Styvaktakis, "The use of time-varying AR model for the characterization of voltage distrubances," in *Proc. IEEE Power Engineering Society Winter Meeting*, vol. 4, Jan. 2000, pp. 2943–2948.

[5] R. Andre-Obrecht, "A new statistical approach for the automatic segmentation of continuous speech signals," *IEEE Trans. Acoust., Speech, Signal Process.*, vol. 36, no. 1, pp. 29–40, Jan. 1988.

[6] D. Tjøstheim, "Autoregressive representation of seismic P-wave signals with an application to the problem of short-period discriminants," *Geophysical Journal of Royal Astronomical Society*, vol. 43, pp. 269–291, 1975.

[7] C. J. Dafis, C. O. Nwankpa, and A. Petropulu, "Analysis of power system transient disturbances using an ESPRIT-based method," in *Proc. IEEE Power Engineering Society Summer Meeting*, Seattle, WA, July 2000.

[8] M. Basseville and I. V. Nikiforov, *Detection of Abrupt Changes: Theory and Application*. Prentice Hall, 1993.

[9] "Alternative transient program website," [Online]. Available: www.emtp.org.